

Domain Dynamics in Quantum-Paraelectric SrTiO₃

Sergey Kustov,¹ Iulia Liubimova,² and Ekhard K. H. Salje^{3,*}

¹*University of Balearic Islands, 07122 Palma de Mallorca, Spain*

²*ITMO University, Kronverksky pr. 49, St. Petersburg 197101, Russia*

³*Cambridge University, CBI 2HG Cambridge, United Kingdom*



(Received 12 August 2019; published 7 January 2020)

Twin dynamics forced by acoustic waves shows several linear and nonlinear response modes below $T_c = 106$ K. In the quantum paraelectric state a “quantum domain glass” at $25 \text{ K} < T < 40 \text{ K}$ shows intense relaxation and temperature hysteresis. Domains float collectively in a complex, smooth landscape with long relaxation times. In the “quantum domain solid” state below 25 K new phenomena occur. A temperature-dependent memory effect of the elastic response after anneal at 36 K depends on the lowest temperature reached in the quantum domain solid state below 25 K. The glassiness of twin boundary dynamics vanishes for temperatures approaching absolute zero.

DOI: [10.1103/PhysRevLett.124.016801](https://doi.org/10.1103/PhysRevLett.124.016801)

SrTiO₃ is a most unusual ferroelastic material sometimes coined the “drosophila of solid state physics” [1]. Its spontaneous strain is small so that other lattice effects superpose the ferroelastic deformation. The additional off-centering of Sr [2] and local cell doubling effects related to antiphase boundaries, APBs, combine with large quantum fluctuations at low temperatures that are sufficient to prevent the ferroelastic phase from becoming ferroelectric [3]. The nature of the quantum state is obscure, however, and the closeness of the quantum critical point [4] gives little information about the dynamical behavior. Various anomalies below 6 K may result from nonphonon excitations [5]. Several such excitations are relevant in SrTiO₃. The first relates to the ferroelastic order parameter associated with the phase transition at $T_c = 106$ K. The second relates to the incipient ferroelectric transition, which couples with the ferroelastic order parameter. Their coupling [6] is expected to be biquadratic and both transitions repel each other [7]. The third low energy excitation is due to APB movements. APBs may trigger ferroelectricity locally [8]. Twin boundaries (TB) also become polar below ~ 60 K. The polarity inside TBs strongly increases first below 45 K with another increase near 20 K [1,9]. All fluctuations contribute to the movement of TBs, which are unusually mobile in SrTiO₃.

The high domain mobility between $T_c = 106$ and 10 K was previously detected using a dynamic mechanical analyzer (DMA) [10], resonant ultrasonic spectroscopy, and resonant piezoelectric spectroscopy [1,9]. No TB freezing was found in SrTiO₃. Instead, twin wall dynamics changes near 43 K on cooling to a glassy dynamics with extremely slow logarithmic relaxations [11]. Direct observations of needle domains and complex domain patterns under driving electric fields [12] show avalanche-type changes with power law distributions of the displacement

amplitudes below 25 K. Avalanches are thermally activated at 45–25 K [12]. Previous experiments focused on separate studies of either linear [1,9,11,13] or nonlinear TB dynamics [10,12]. The transition from linear to nonlinear dynamics, i.e., the emergence and type of the nonlinearity, is a hallmark of the quantum TB state in SrTiO₃. In this work we scan the applied strains starting at a lower limit $\sim 10^{-8}$ to ca. 10^{-6} . The low strain limit permits detecting possible transitions from linear to non-linear TB dynamics and to capture the anomalies of the TB states.

We measured the acoustic response from resonant standing waves—the elastic stiffness and the ultrasonic absorption (internal friction, IF) at 90 kHz vs temperature and oscillatory strain amplitude ϵ_0 . Temperature spectra were registered at a low $\epsilon_0 = 10^{-7}$ to reduce the contribution of the nonlinear acoustic effects. Strain amplitude dependences were registered at several temperatures during heating for ϵ_0 between 2×10^{-8} and ca. 10^{-6} . During these measurements, ϵ_0 was first increased with a preset step (10%) up to a maximum value (direct run) and then decreased in the inverse sequence (reverse run). Details of the experimental method and of determination of the Young’s modulus, E , and IF of the sample can be found in Refs. [14–16].

The effect of temperature for low amplitudes of TB dynamics is shown by the IF, δ , and the Young’s modulus E in Figs. 1(a) and 1(b). The ferroelastic transition at $T_c \approx 106$ K [18,19] is seen as a sharp drop in E and a weak peak in δ , as is typical for ferroelastic phase transitions [20]. The IF peak near 90 K, similar to Ref. [21], is not related to the phase transition: its position at 90 kHz agrees with an Arrhenius-type relaxation (activation energy 0.12 eV, frequency factor 2×10^{11} Hz) reported for dielectric properties [22]. No corresponding change of the Young’s modulus is seen at 90 K, since it is dwarfed by the massive softening

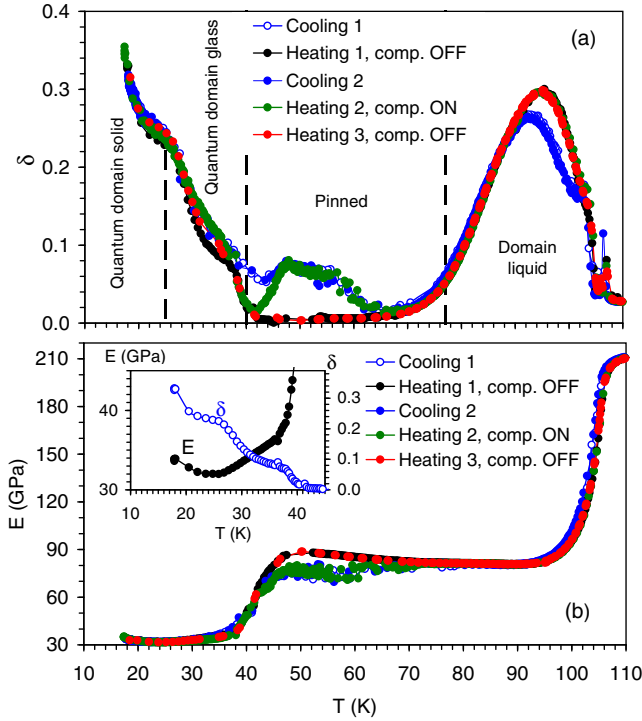


FIG. 1. Temperature spectra of low-amplitude ($\epsilon_0 = 10^{-7}$) ultrasonic internal friction δ (a) and Young's modulus E (b) for several cooling-heating scans below $T_c \approx 106$ K. Cooling and Heating 2 scans are performed with the cryocompressor switched on, Heating 1 and Heating 3—with the compressor switched off. During Heating 3, strain amplitude dependences of the internal friction were measured at selected temperatures (data shown in Fig. 2). The inset in (b) shows, on an expanded scale, the internal friction δ and Young's modulus E below 40 K during the Heating 1 scan. For the Heating 2 scan (green curve) only each fourth experimental point is shown above 90 K in (a) and (b) to make the points of Heating 1 scan (black curve) visible.

(ca. 60%) during the phase transition. Spectra between 80 and 45 K are dominated by instabilities (jerks) even for low strains of $\epsilon_0 \sim 10^{-7}$. The instabilities persist during cooling and during heating as long as the cryomotor is running and disappear if the cryomotor is switched off. Figure 1 shows that the IF is much higher and the modulus is notably lower in the jerky state compared to smooth spectra with the cryomotor switched off. Therefore, instabilities are related to depinning of TB by weak mechanical vibrations. No thermal hysteresis of the jerky part of the spectra is observed.

The massive softening near 45 K, Fig. 1(b), as reviewed by Lemanov [23], strongly diminishes when the frequency rises from sonic to ca. 10^2 MHz, which is only possible if the nanostructural changes involve highly mobile twins with mobilities greater than their mobility at, say, 60 K. Few other ferroelastic materials display such “inverse” behavior: lowering temperature leads to an increase of domain mobilities for small strain amplitudes due to depinning of TBs by thermal stresses [24]. Below 43 K

the IF and the Young's modulus show three anomalies at 35, 25, and below 17 K [Fig. 1(a), inset in Fig. 1(b)]. The onset of the Young's modulus increase coincides with a 25 K anomaly in the IF spectra [Fig. 1(b)]. The thermal hysteresis between cooling and heating is seen near 30 K and vanishes at 43 K, cf. blue and green curves in Fig. 1(a).

Qualitatively new information on TB dynamics provides the IF dependence on strain amplitude (examples in Fig. 2) which was registered during heating scans in Fig. 1. Figure 2 shows clear breaks in the TB dynamics. $\delta(\epsilon_0)$ near the 90 K relaxation peak (between 105 and 80 K) in Fig. 2(a) shows a linear behavior. In contrast, jerky damping occurs at lower temperatures between 70 and 40 K [Fig. 2(b)] above a critical depinning strain $\epsilon_0^{cr} \approx (2 - 3) \times 10^{-7}$. The jerky TB depinning between 40 and 70 K accounts for unexplained instabilities of the mechanical response beyond critical driving excitation, already reported by Sorge *et al.* [25]. The jerky depinning pattern in SrTiO₃ is similar to recent observations in LaAlO₃ [26]. A remarkable property of TBs in SrTiO₃ is their extremely low depinning strain $\epsilon_0^{cr} \approx 2 \times 10^{-7}$ which is ~ 300 times lower than in LaAlO₃. The depinning stress in SrTiO₃ is $\sigma_0^{cr} = E\epsilon_0^{cr} \approx 0.02$ MPa, so that even the vibrations of the cryomotor are sufficient to depin TBs. $\delta(\epsilon_0)$ scans between 40 and 70 K show a pronounced amplitude hysteresis: the IF during increasing ϵ_0 is lower than during decreasing ϵ_0 . This amplitude hysteresis reflects a rearrangement of the pinning centers by oscillating TBs [27] proving the mobility of pinners. Strain amplitude hysteresis diminishes when the temperature rises to ca. 70 K [Fig. 2(b)]. Hence, the relaxation time of the pinning potential disturbed by oscillating TBs becomes less than the time of measurements of a strain dependence (ca. 60 s) due to an increase of the mobility of pinning centers.

At higher temperatures, nonlinear depinning transforms gradually to linear IF concomitant with the appearance of a relaxation peak. This scenario is typical for the transition from the depinning mode to dragging of mobile pinners [28]. Below the depinning range, $T < 40$ K, the damping raises sharply and the nonlinear TB response switches abruptly from jerky to continuous. $\delta(\epsilon_0)$ below 40 K is nonlinear over the entire strain amplitude range in Fig. 2(c). This property is typical for glassy dynamics [29–31] due to divergence of the barrier height with decreasing strain amplitudes [30,31]. The observed onset of the glassy dynamics coincides with the high polarity of the twin boundaries and the onset of the glassy twin dynamics seen by electric field driven experiments [32]. $\delta(\epsilon_0)$ below ca. 40 K follows a power law with the glassy exponent μ : $\delta(\epsilon_0) \propto (\epsilon_0)^\mu$. Figure 2(d) shows that μ decreases sharply below 30 K from ca. 0.6 to 0.2. The former value is close to (0.5–0.6) reported for glassy dynamics of defects in faulted martensites [31]. In contrast to the temperature independence of the glassy exponent in Ref. [33], the value of μ in SrTiO₃ vanishes for $T \rightarrow 0$ K as shows the inset in Fig. 2(d).

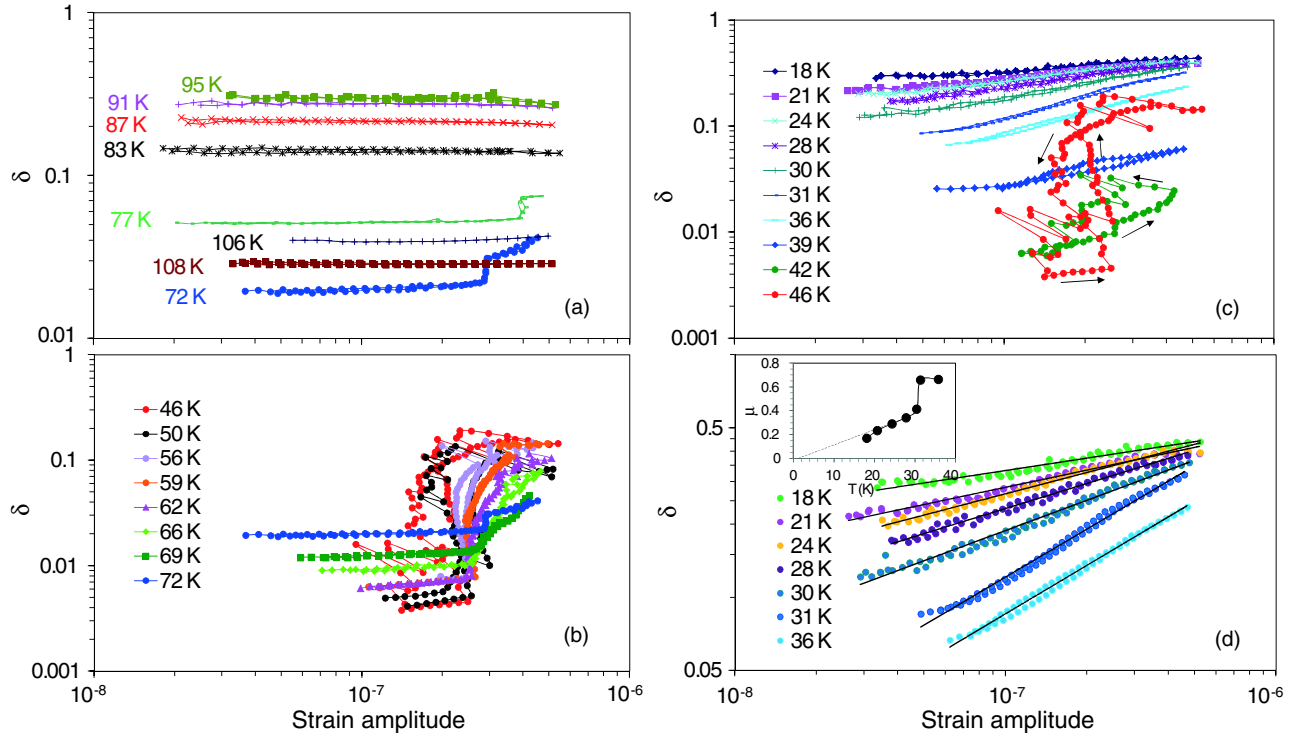


FIG. 2. Strain amplitude dependence of the internal friction δ measured at temperatures between 72 and 108 K (a), 46 and 72 K (b), and 18 and 46 K (c) during heating from 18 K. Solid lines connect experimental points in panels (a),(b), and (c). All strain amplitude dependences include direct and reverse runs (increasing and decreasing strain amplitude). The jerks during increasing and decreasing strain amplitudes are seen in (b) and (c). Arrows in Fig. 2(c) (for jerky curves at 42 and 46 K) indicate increase and decrease of the strain amplitude, mark the difference between the data for direct and reverse runs, and indicate the strain amplitude hysteresis between ca. 40 and 70 K. Panel (d) shows the strain amplitude dependences between 18 and 36 K on an expanded scale. Solid lines are their fittings with power law. The inset shows the glassy strain exponent μ vs temperature; the dotted line in the inset is a guide to the eye.

The existence of a memory effect in E and IF, typical for glassy systems, was established following the protocol in Fig. 3(a). The sample was cooled initially to various minimum temperatures $T_{\min 1}$ between 17 and 36 K. Then the sample was heated to the annealing temperature $T_{\text{anneal}} = 36$ K and kept at this temperature during 2 h. For $T_{\min 1} = T_{\text{anneal}} = 36$ K the annealing was performed during the interruption of a cooling run. The annealing was followed by cooling the sample to the lowest temperature of 17 K. The memory effect was then checked during subsequent heating of the sample.

Figure 3(b) shows the Young’s modulus during a continuous cooling-heating cycle. Figures 3(c)–3(g) indicate that the key ingredient for the memory effect is the direction of the approach to annealing and the lowest temperature reached before annealing at 36 K. Annealing the sample during cooling (for $T_{\min 1} = T_{\text{anneal}}$) does not produce any memory effect [Fig. 3(c)]. In contrast, pre-cooling the sample below 25 K before annealing at $T_{\text{anneal}} = 36$ K results in a complete memory effect; i.e., the annealed state at 36 K is fully recovered when reheating from 17 K [Fig. 3(d)]. Figures 3(e)–3(g) show the memory effect for different precooling temperatures $T_{\min 1}$. The overall results are summarized in Fig. 3(h).

The memory effect changes dramatically at $T_{\min 1} = 25$ K. Cooling the sample below 25 K affects its annealing behavior at 36 K and structural changes introduced below 25 K are at least partially maintained at higher temperatures. This result is consistent with observations of thermal hysteresis in linear IF between cooling and heating that emerges around 30 K and vanishes completely at 45 K [Fig. 1(a)]. Temperature hysteresis also indicates that the changes of the quantum paraelectric state introduced by cooling below 25 K persist at higher temperatures up to 45 K.

Our study of linear *and* nonlinear acoustic properties of SrTiO₃ allows us to identify temperature ranges of distinct types of TB dynamics and, most importantly, reveals potentially a new state of TBs in the quantum paraelectric phase below ca. 25 K. The main types of the TB dynamics between T_c and 17 K are represented by a summary of strain amplitude dependences in Fig. 4. Corresponding temperature ranges are shown schematically in Fig. 1(a). At elevated temperatures between T_c and ca. 70 K TB motion corresponds to linear viscous flow of unpinned TBs (or the “domain liquid” state), presumably characterized by sufficient mobility of pinning centers. $\delta(\epsilon_0)$ measured at 56 K exemplifies pinned states and thermally activated depinning by oscillatory stress operating between 70 and 40 K. The

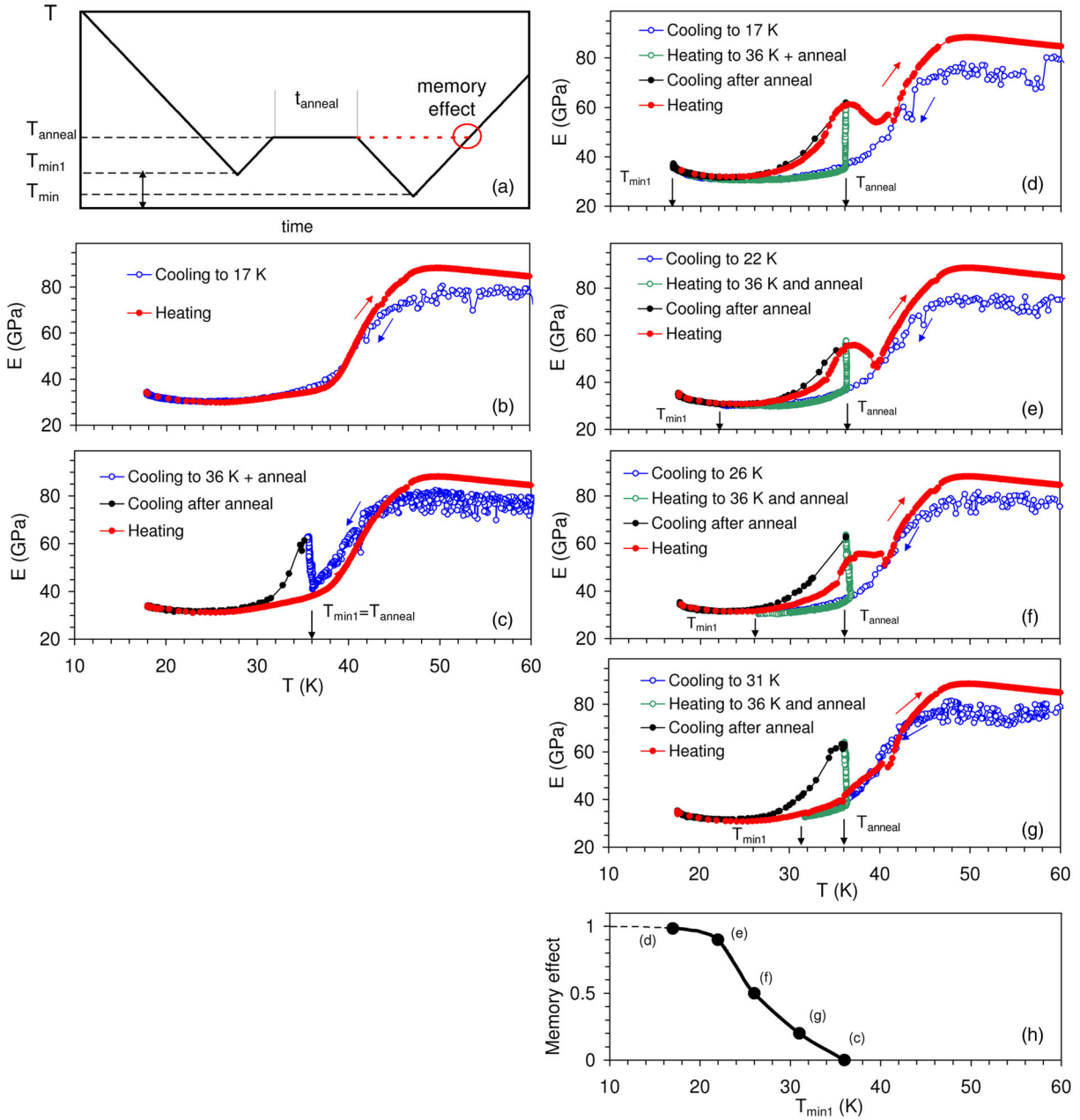


FIG. 3. (a) Schematic time-temperature diagram of experimental protocol used to study the “memory” effect in the temperature spectra of Young’s modulus, induced by annealing the sample at a temperature T_{anneal} , which includes (i) cooling from above T_c to a variable temperature $T_{\min 1}$, (ii) heating to a temperature T_{anneal} and isothermal holding at T_{anneal} during time t_{anneal} , (iii) cooling to $T_{\min} = 17$ K and (iv) heating above T_c . (b) Young’s modulus E vs temperature for the continuous cooling-heating cycle; (c) annealing experiment following the protocol in Fig. 3(a) with $T_{\min 1} = T_{\text{anneal}} = 36$ K; (d),(e),(f), and (g) annealing experiments following the same protocol with $T_{\min 1} = 17, 22, 26,$ and 31 K, respectively, $T_{\text{anneal}} = 36$ K and $t_{\text{anneal}} = 2$ h. Panel (h) shows the fraction of the Young’s modulus increase during isothermal annealing recovered as “memory effect” during consecutive heating as a function of the temperature of precooling $T_{\min 1}$; letters (c),(d),(e),(f), and (g) close to the data points denote the panels from which the data were taken.

glassy state of TB motion below 40 K is demonstrated by $\delta(\epsilon_0)$ taken at 30 K with an intermediate value of the glassy exponent $\mu \approx 0.4$. Several observations point to the existence of a new state of TBs in the quantum paraelectric phase below ca. 25 K.

First, it is known that in SrTiO_3 the domain glass below ca. 40 K is not an equilibrium state [11]. The latter corresponds

to higher modulus values and the relaxation time of domain glass towards the equilibrium state under distinct types of excitation diverges rapidly around 30 K [11].

Second, we observe a sharp decrease of the glassy exponent below 25 K that vanishes for $T \rightarrow 0$ K. This effect can be rationalized by the idea that the glassy exponent μ measures the divergence of energy barriers

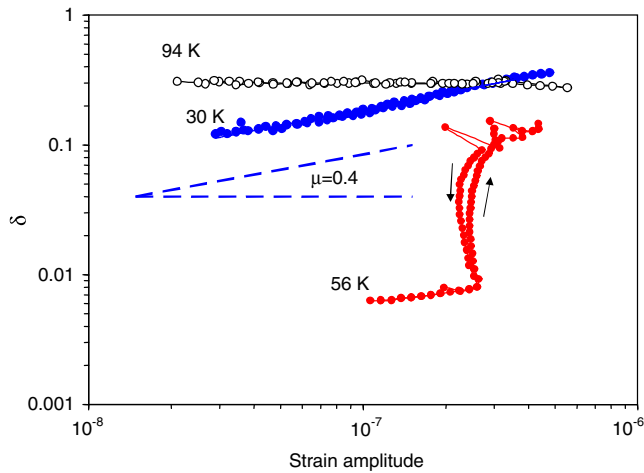


FIG. 4. Examples of strain amplitude dependences of the internal friction δ for selected temperatures of 94, 56, and 30 K, representative for viscous twin boundary motion, depinning, and glassy dynamics, respectively.

for $\varepsilon \rightarrow 0$ [30,31] and $\mu \rightarrow 0$ implies, thus, a reduction of barriers and transition to linear TB dynamics. Quite remarkable are similar values of δ for unpinned TBs around 90 K (i.e., outside the quantum paraelectric region) and at the lowest temperatures, Figs. 2(a) and 2(c).

Third, the linearization of the IF is accompanied by elastic stiffening. The Young's modulus increases compared with the glassy state, as shown in the inset of Fig. 1(b), tending towards equilibrium values of the Young's modulus.

Fourth, the temperature around 25 K indicates a transition from the complete to a vanishing memory effect, Fig. 3(h). Only after reaching this new state, the relaxation of the domain glass at 36 K towards equilibrium results in a memory effect.

The above arguments point to a transition below ca. 25 K of a domain glass to a new state, with less glassiness, higher stiffness, nearly linear TB dynamics and completely frozen TB relaxation. All these features are characteristic of a domain solid state. Since SrTiO₃ below 50 K is in a quantum critical state, on the border of ferroelectric transition [4], we suggest referring to this state as “quantum domain solid,” in contrast to a “quantum domain glass” between ca. 45 and 30 K [11]. A transition to quantum domain solid corresponds to (i) decreasing glassiness, hence, more ordered state of TBs, and (ii) approaching classical linear TB dynamics. This result chimes with the notion of a “coherent quantum state” in SrTiO₃ as first formulated by Müller *et al.* [34].

The work was supported by Spanish Ministerio de Ciencia, Innovación y Universidades-Agencia Estatal de Innovación and FEDER, UE (Project No. RTI 2018-094683-B-C51) and by the Ministry of Science and

Higher Education of the Russian Federation, goszadanie No. 3.1421.2017/4.6. E. K. H. S. is grateful to EPSRC (EP/P024904/1) and the Leverhulme trust (EM-2016-004).

*Corresponding author.

ekhard@esc.cam.ac.uk

- [1] E. K. H. Salje, O. Aktas, M. A. Carpenter, V. V. Laguta, and J. F. Scott, Domains within Domains and Walls within Walls: Evidence for Polar Domains in Cryogenic SrTiO₃, *Phys. Rev. Lett.* **111**, 247603 (2013).
- [2] R. Blinc, B. C. V. Zalar, V. V. Laguta, and M. Itoh, Order-Disorder Component in the Phase Transition Mechanism of O-18 Enriched Strontium Titanate, *Phys. Rev. Lett.* **94**, 147601 (2005).
- [3] J. H. Barrett, Dielectric constant in perovskite type crystals, *Phys. Rev.* **86**, 118 (1952); K. A. Müller and H. Burkhard, SrTiO₃: An intrinsic quantum paraelectric below 4 K, *Phys. Rev. B* **19**, 3593 (1979); E. K. H. Salje, B. Wruck, and H. Thomas, Order-parameter saturation and low-temperature extension of Landau theory, *Z. Phys. B Condens. Matter* **82**, 399 (1991); O. E. Kvyatkovskii, Quantum effects in incipient and low-temperature ferroelectrics, *Phys. Solid State* **43**, 1401 (2001).
- [4] S. E. Rowley, L. J. Spalek, R. P. Smith, M. P. M. Dean, M. Itoh, J. F. Scott, G. G. Lonzarich, and S. S. Saxena, Ferroelectric quantum criticality, *Nat. Phys.* **10**, 367 (2014).
- [5] S. Conti, S. Mueller, A. Poliakovsky, and E. K. H. Salje, Coupling of order parameters, chirality, and interfacial structures in multiferroic materials, *J. Phys. Condens. Matter* **23**, 142203 (2011).
- [6] B. Houchmandzadeh, J. Lajzerowicz, and E. K. H. Salje, Order parameter coupling and chirality of domain-walls, *J. Phys. Condens. Matter* **3**, 5163 (1991).
- [7] E. Golovenchits, V. Sanina, and A. Babinsky, Nonlinear dielectric susceptibility and the possible origin of the low temperature state of SrTiO₃, *Ferroelectrics* **199**, 317 (1997).
- [8] M. Stengel (private communication).
- [9] J. F. Scott, E. K. H. Salje, and M. A. Carpenter, Domain Wall Damping and Elastic Softening in SrTiO₃: Evidence for Polar Twin Walls, *Phys. Rev. Lett.* **109**, 187601 (2012).
- [10] A. V. Kityk, W. Schranz, P. Sondergeld, D. Havlik, E. K. H. Salje, and J. F. Scott, Low-frequency superelasticity and nonlinear elastic behavior of SrTiO₃ crystals, *Phys. Rev. B* **61**, 946 (2000).
- [11] D. Pesquera, M. A. Carpenter, and E. K. H. Salje, Glasslike Dynamics of Polar Domain Walls in Cryogenic SrTiO₃, *Phys. Rev. Lett.* **121**, 235701 (2018).
- [12] B. Casals, S. Van Dijken, G. Herranz, and E. K. H. Salje, Electric field induced avalanches and glassiness of mobile ferroelastic twin domains in cryogenic SrTiO₃, *Phys. Rev. Res.* **1**, 032025(R) (2019).
- [13] E. V. Balashova, V. V. Lemanov, R. Kunze, G. Martin, and M. Weihnacht, Ultrasonic study on the tetragonal and Müller phase in SrTiO₃, *Ferroelectrics* **183**, 75 (1996).
- [14] W. H. Robinson and A. Edgar, The piezoelectric method of determining mechanical damping at frequencies of 30 to 200 kHz, *IEEE Trans. Sonics Ultrasonics* **SU-21**, 98 (1974).

- [15] S. Kustov, S. Golyandin, A. Ichino, and G. Gremaud, A new design of automated piezoelectric composite oscillator technique, *Mater. Sci. Eng. A* **442**, 532 (2006).
- [16] See Supplemental Material at <http://link.aps.org/supplemental/10.1103/PhysRevLett.124.016801> for details of sample preparation and the method of Young's modulus determination from the resonant frequency of the oscillator, which includes Ref. [17].
- [17] T. A. Read, The internal friction of single metal crystals, *Phys. Rev.* **58**, 371 (1940).
- [18] R. O. Bell and G. Rupprecht, Elastic constants of strontium titanate, *Phys. Rev.* **129**, 90 (1963).
- [19] K. Fossheim and B. Berre, Ultrasonic propagation, stress effects, and interaction parameters at the displacive transition in SrTiO₃, *Phys. Rev. B* **5**, 3292 (1972).
- [20] E. K. H. Salje, Ferroelastic materials, *Annu. Rev. Mater. Res.* **42**, 265 (2012).
- [21] O.-M. Nes, K. A. Müller, T. Suzuki, and F. Fossheim, Elastic anomalies in the quantum paraelectric regime of SrTiO₃, *Europhys. Lett.* **19**, 397 (1992).
- [22] R. Viana, P. Lunkenheimer, J. Hemberger, R. Böhmer, and A. Loidl, Dielectric spectroscopy in SrTiO₃, *Phys. Rev. B* **50**, 601 (1994).
- [23] V. V. Lemanov, Improper ferroelastic SrTiO₃ and what we know today about its properties, *Ferroelectrics* **265**, 1 (2002).
- [24] S. Kustov, S. Golyandin, K. Sapozhnikov, J. Van Humbeeck, and R. De Batist, Low-temperature anomalies in Young's modulus and internal friction of Cu-Al-Ni single crystals, *Acta Mater.* **46**, 5117 (1998).
- [25] G. Sorge, E. Hegenbarth, and G. Schmidt, Mechanical relaxation and nonlinearity in strontium titanate single crystals, *Phys. Status Solidi* **37**, 599 (1970).
- [26] S. Kustov, Iu. Liubimova, and E. K. H. Salje, LaAlO₃: A substrate material with unusual ferroelastic properties, *Appl. Phys. Lett.* **112**, 042902 (2018).
- [27] S. Kustov, K. Sapozhnikov, and X. Wang, Phenomena associated with diffusion, assisted by moving interfaces in shape memory alloys, *Funct. Mater. Lett.* **10**, 1740010 (2017).
- [28] G. Gremaud, Dislocation point defect interaction, *Mater. Sci. Forum* **366**, 178 (2001).
- [29] S. Kustov, E. Cesari, and G. Gremaud, Non-linear anelasticity of topological vortex matter in martensites, *Mater. Sci. Eng. A* **442**, 390 (2006); Glassy and liquid vortex matter dynamics in faulted martensites, *Mater. Sci. Eng. A* **481–482**, 28 (2008).
- [30] G. Blatter, M. V. Feigelman, V. B. Geshkenbein, A. I. Larkin, and V. M. Vinokur, Vortices in high-temperature superconductors, *Rev. Mod. Phys.* **66**, 1125 (1994).
- [31] G. D'Anna, W. Benoit, and V. M. Vinokur, Internal friction and dislocation collective pinning in disordered quenched solid solutions, *J. Appl. Phys.* **82**, 5983 (1997).
- [32] G. Lu, S. Li, X. Ding, and E. K. H. Salje, Piezoelectricity and electrostriction in ferroelastic materials with polar twin boundaries and domain junctions, *Appl. Phys. Lett.* **114**, 202901 (2019).
- [33] J. Van Humbeeck and S. Kustov, Active and passive damping of noise and vibrations through shape memory alloys: Applications, and mechanisms, *Smart Mater. Struct.* **14**, S171 (2005).
- [34] K. A. Müller, W. Berlinger, and E. Tosatti, Indication for a novel phase in the quantum paraelectric regime of SrTiO₃, *Z. Phys. B* **84**, 277 (1991).